Determination of AC–DC Difference in the 0.1–100 MHz Frequency Range

JOSEPH R. KINARD, SENIOR MEMBER, IEEE, AND TI-XIONG CAI

Abstract—Thermal voltage converter structures have been modeled theoretically and studied experimentally to determine their ac–dc differences in the 0.1–100 MHz frequency range. Estimated uncertainties, corresponding to the one standard deviation confidence level, for these ac–dc differences vary from 20 ppm at 1 MHz to 2000 ppm at 100 MHz.

I. Introduction

In THE frequency range of 100 kHz–100 MHz, ac voltage measurements of the highest accuracy are generally made using thermal voltage converters (TVC's) constructed with thermoelements (TE's) and series resistors mounted on the axis of a cylindrical structure.

This paper describes theoretical and experimental methods for the determination of the ac–dc differences for a group of thermal voltage converters emphasizing the 10 to 25 V ranges having series resistors ranging from 1 to 5 kΩ. The design and materials used in the construction of these TVC's were chosen in order to permit detailed modeling and analysis. The major contributions to ac–dc difference, for the 10–25-V converters under study in this work, were:

a) the voltage standing wave in the input connector and tee structure, point p to point q in Fig. 1, since all TVC's considered here are relatively high-impedance nonmatching loads;
b) the transimpedance, the ratio of the voltage at point q to the current flowing out of the series resistor section, Region 1 in Fig. 1;
c) the current standing wave in the thermoelement section, Region 2 in Fig. 1;
d) to a lesser extent, skin effect in the overall structure.

Of these, a) and c) are essentially voltage range independent for the 10–25 V ranges. Intercomparisons of different voltage ranges will not necessarily reveal the presence of a) and c), so fairly elaborate analyses and measurements, as described below, were required to assign values to these effects. Contributions b) and d) are essentially range dependent, so that, in general, intercomparisons of properly constructed TVC's of different voltage ranges will reveal their presence and allow them to be evaluated.

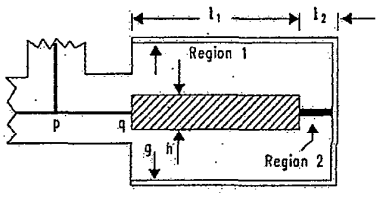

Fig. 1. Diagram of TVC structure. The input tee and connector are shown at positions p and q, respectively. The range resistor is given as Region 1 and the thermoelement is given as Region 2.

II. Description of Converters and Comparator System

The TVC's studied included some described by Hermach and Williams [1] as well as newly constructed converters of a similar design. All of the converters contained UHF-type thermoelements, rated from 2.5 to 10 mA, with heaters and feedthroughs colinear. To reduce coupling, the thermocouple leads were taken out of the TE in a plane perpendicular to the heater. Some of the new TVC's contained specially constructed thermoelements made with Evanohm heaters and platinum iridium feedthrough leads instead of the usual magnetic dumet leads. All of the new converters were constructed entirely of nonmagnetic material to minimize skin effect. The converter cylinders and the input connectors were constructed mostly of brass. The series resistors were cylindrical ceramic rods with an unspiraled deposited carbon coating. The manufacturer's original glass encapsulation, magnetic end caps, and leads were removed and replaced with copper end caps and leads as shown in Fig. 2.

For the newly constructed converters, the TE's were first intercompared as current converters over the entire frequency range. Some of these measurements on the TE's were made with the two elements mounted in series on the axis of a cylinder. The input signal was applied alternately at one end and then the other, with the opposite end short circuited. A detailed analysis of this method at frequencies above 1 MHz is given in a later part of this paper. Other intercomparisons were made by carefully in-

Manuscript received June 10, 1988. This work was partially supported by the Calibration Coordination Group of the U.S. Department of Defense.

J. R. Kinard is with the National Bureau of Standards, Electricity Division, Gaithersburg, MD 20899.

T.-X. Cai is with the National Bureau of Standards, Electricity Division, Gaithersburg, MD 20899, on leave from the Shanghai Institute of Testing Technology, Radio Department, Shanghai, China.

IEEE Log Number 8826200.

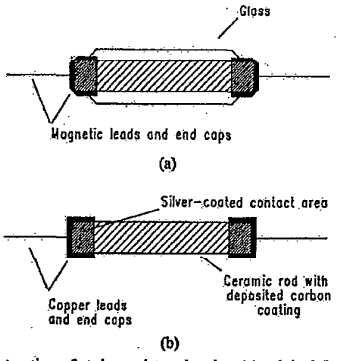

Fig. 2. Construction of series resistor showing (a) original form and (b) modified form.

terchanging TE's in a 10–20-V range converter structure. TE's selected for use had generally negligible variations in ac–dc difference as current converters compared to the overall uncertainties at the various frequencies.

The improvements in the characterization of TVC's in this frequency range were made possible, in part, by the use of a high-performance semiautomated comparator system as shown in Fig. 3. The system contains an RF signal source, broad-band power amplifier, reversible dc power supply, coaxial ac–dc relay switch, Lindeck potentiometer, resistance divider network, digital nanovoltmeter, and desktop computer. Comparisons were made in the usual way by connecting the TVC's in parallel, with a coaxial tee employing the common type of connector used on TVC's in this frequency range, type 874. Data were taken at equal time intervals using the sequence ac, dc+, dc−, ac. The output of one TVC designated test, was held constant during an ac–dc difference comparison by the use of the Lindeck potentiometer and the fine adjustments on the sources. The ac fine control consisted of a small finely adjustable dc voltage applied as external amplitude modulation to the RF signal generator.

The larger of the two TE outputs was nulled directly against the smaller using the 4.9-kΩ resistive divider. Overall system timing, data collection, and data reduction from the digital nanovoltmeter were provided by the desktop computer. Standard deviations of only a few parts per million were obtained for a group of ac–dc difference measurements over the whole frequency range.

III. Frequency Range of 1–100 MHz

The frequency range of 0.1–100 MHz may be considered as two separate frequency regions requiring related but different approaches. The division of the frequency range into two regions is appropriate because the range-independent contributions to ac–dc difference are found to be generally negligible from 0.1 to 1 MHz, and the TVC's can be made so that the range-dependent contributions are comparable to the uncertainties arising from the ability to define and intercompare the TVC's. The frequency range of 0.1–1 MHz is discussed in a later section. In the frequency region of 1 to 100 MHz, all the range-independent as well as range-dependent contributions to ac–dc difference are important. Each of these contributions was analyzed and its value calculated or measured as described in the following sections.

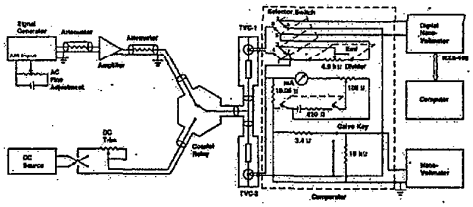

Fig. 3. AC–DC difference comparator system

A. Voltage Standing Wave Contribution

As a practical convenience TVC's are made with coaxial input connectors, and it is common practice to define the ac–dc differences for TVC's with reference to the midpoint plane of a coaxial tee mated to the input connector structure. For this investigation all the TVC's were constructed using type 874 connectors and, except where noted otherwise, all intercomparisons and ac–dc difference values are referenced to the midpoint plane of a type 874 tee. A range-independent ac–dc difference arises from the voltage standing wave in this input connector and tee structure. Since the characteristic impedance (hundreds of ohms or more) of the main body of the converter structure is much higher than the nominal 50-Ω characteristic impedance for the tee and input connector, the voltage at plane q in Fig. 1, can differ significantly from that at plane p. For this analysis, the tee structure and input connector will be approximated as a uniform loss-free transmission line. Defects in the construction of the 874 tee and connector appear as corrections or second-order terms to this approximation.

With Z as the total series impedance and Y as the total shunt admittance in the transmission line between p and q, the transmission line formulas [2] give

$$V_p = V_q \cosh \gamma + I_q Z_0 \sinh \gamma$$

where

$$\gamma = (ZY)^{1/2}, \qquad Z_0 = \left(\frac{Z}{Y}\right)^{1/2}.$$

But

$$I_q = \frac{V_q}{Z_1}, \qquad Z_0 = \frac{Z}{\gamma}$$

where Z_1 is the input impedance in Region 1 of Fig. 1, so

$$V_p = V_q \left(\cosh \gamma + \frac{Z}{Z_1} \frac{\sinh \gamma}{\gamma}\right).$$

Expanding the hyperbolic functions gives

$$\frac{V_p}{V_q} = 1 + \frac{\gamma^2}{2} + \frac{Z}{Z_1} + \frac{Z}{Z_1}\frac{\gamma^2}{6} + \cdots$$

with

$$\gamma = j\omega CZ_0, \quad \gamma^2 = -(\omega CZ_0)^2, \quad Z = j\omega CZ_0^2$$

so

$$\frac{V_p}{V_q} = 1 - \frac{(\omega CZ_0)^2}{2} + j\frac{\omega CZ_0^2}{Z_1} - j\frac{\omega CZ_0^2}{6Z_1}(\omega CZ_0)^2.$$

By letting $\alpha = \omega CZ_0$, $M = Z_0/Z_1$, and since $\alpha \ll 1$, if $Z_1 = R_1$:

$$\frac{V_p}{V_q} = 1 - \frac{\alpha^2}{2} + j\alpha M - j\frac{\alpha^3 M}{6}.$$

Dropping the higher order term and taking the magnitude gives

$$\frac{V_p}{V_q} = \left[\left(1 - \frac{\alpha^2}{2}\right)^2 + (\alpha M)^2\right]^{1/2} \simeq 1 - \frac{\alpha^2}{2}(1 - M^2).$$

Thus the ac–dc difference contribution from the coaxial connector and tee is

$$\delta_c \simeq -\frac{\alpha^2}{2}(1 - M^2). \tag{1}$$

The parameters α and M were determined from the geometric dimensions of the tee structure and input connector and from the value of R_1. The contribution to ac–dc difference predicted by (1) was tested by using a specially constructed TVC with an input connection brought in at plane q. The results shown in Fig. 4 confirm the very good agreement between the model, plotted as the solid line, and measured values indicated by diamonds.

B. Transimpedance Contribution

The second major contribution to ac–dc difference, which is also the main range-dependent component, is due to the transimpedance of the part of the TVC structure containing the series range resistor, labeled Region 1 in Fig. 1. This region may be represented as a transmission line [2], [3] with a uniformly distributed series impedance of Z_1 Ω per unit length, distributed shunt admittance of Y_1 S per unit length, and overall length l_1. The transimpedance is $Z_{tr} = V_{in}/I_h$, where V_{in} is the input voltage at plane q and I_h is the current flowing into the heater, or Region 2. The ac–dc difference contribution from this region can be written as $\delta_{tr} = (|Z_{tr}| - R_t)/R_t$ where R_t is the dc value of the series resistor plus heater resistance. For the transmission line of Region 1, Fig. 1, terminated in a TE heater resistance, R_h:

$$Z_{tr} = R_h \cosh\sqrt{Z_1 Y_1} + \frac{Z_1}{\sqrt{Z_1 Y_1}}\sinh\sqrt{Z_1 Y_1}. \tag{2}$$

The thermoelement in Region 2 of Fig. 1 may be represented as a short circuited transmission line with input impedance Z_h given by

$$Z_h = \frac{Z_2}{\sqrt{Z_2 Y_2}}\tanh\sqrt{Z_2 Y_2}.$$

Substituting Z_h for R_h in (2) gives the complete expression for the transimpedance of Region 1:

$$Z_{tr} = \frac{Z_2}{\sqrt{Z_2 Y_2}}\tanh\sqrt{Z_2 Y_2}\cosh\sqrt{Z_1 Y_1} + \frac{Z_1}{\sqrt{Z_1 Y_1}}\sinh\sqrt{Z_1 Y_1}.$$

This yields the following expression for ac–dc difference from reactance effects of

$$\delta_{tr} = \frac{a_1^2}{2(1+m)^2}\left[(K_1 + mK_2)^2 - AK_1 + CK_2 + \frac{B}{6}\right]$$

$$K_1 = \frac{b_1}{a_1}, \quad K_2 = \frac{b_2}{a_1}, \quad m = \frac{R_2}{R_1}, \quad n = \frac{a_2}{a_1}$$

$$A = \left(m^2 + \frac{2}{3}m + \frac{1}{3}\right), \quad B = \left(m^2 + \frac{2}{5}m + \frac{1}{15}\right)$$

$$C = \frac{4}{3}m\left(nm + n - \frac{1}{2}\right)$$

with $a_i \ll 1$ and $b_i \ll 1$, where $a_i = \omega C_i R_i$, $b = \omega L_i/R_i$, and C_i, R_i, and L_i are the total capacitance, resistance, and inductance for the respective regions, either 1 or 2 in Fig. 1.

The model described above for this major range-dependent contribution to ac–dc difference was tested by inter-

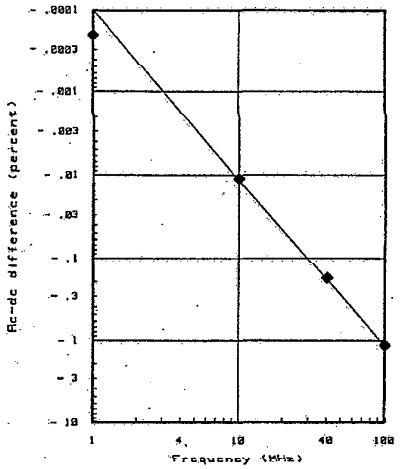

Fig. 4. Calculated values for input tee and connector voltage standing wave contribution to ac–dc difference shown as solid line. Measured points shown as diamonds.

comparison of three specially constructed TVC's having parameters as follows:

	I	R_1
TVC_1	10 mA	1.1 kΩ
TVC_2	5 mA	2.1 kΩ
TVC_3	2.5 mA	5.6 kΩ

As mentioned in [1], the effective length of the resistor is longer than its physical length due to the fringing field at the ends. Based on determinations in [1], an increase in length of 20 percent was used for the calculations of the total capacitance and inductance in Region 1, Fig. 1. The results showing the excellent agreement between calculated values, plotted as lines, and measured values, indicated as diamonds, are given in Fig. 5. Not shown in Fig. 5 is a measured value for TVC_2 versus TVC_1 of approximately −3 ppm at 1 MHz.

C. Current Standing Wave Contribution

The next contribution to ac–dc difference, like the previous two, also becomes significant at frequencies above 1 MHz. For this frequency region the current across the thermoelement heater structure varies significantly due to the current standing wave in this part of the transmission line. To determine the value of this effect, two TE's were placed in series in a coaxial structure, and relative ac–dc difference determinations were made by first shorting one end of the structure with the voltage applied to the other, and then by interchanging the shorted and input ends. The schematic diagram in Fig. 6 shows a cross section of the arrangement used for these measurements. From transmission line formulas [2], the current at a point x on the axis in a transmission line with a short circuit at $x = 0$ is given by

$$I_x = I_r \cosh \alpha x$$

where I_r is the current at the short circuit and $\alpha = \sqrt{Z_u Y_u}$. Z_u is the series impedance ($Z_u = R_u + j\omega L_u$) per unit length, and Y_u is the shunt admittance ($Y_u = G_u + j\omega C_u$) per unit length. This portion of the transmission line is assumed to be lossless, so G_u is taken to be negligible. By expanding the hyperbolic cosine function, and noting that $\omega C_u R_u \ll 1$ and $\omega^2 L_u C_u \ll 1$, the expression for the magnitude of I_x becomes

$$I_x \approx I_r \left(1 + \frac{(\omega C_u R_u)^2 x^4}{12} - \frac{(\omega^2 L_u C_u) x^2}{2}\right)$$

neglecting higher order terms.

Due to the coaxial geometry of the structure, the resistance values of typical thermoelements, and the TE heater dimensions, $(C_u R_u^2) \ll L_u$ for each portion of this part of the transmission line, so

$$I_x = I_r(1 - k\omega^2 x^2)$$

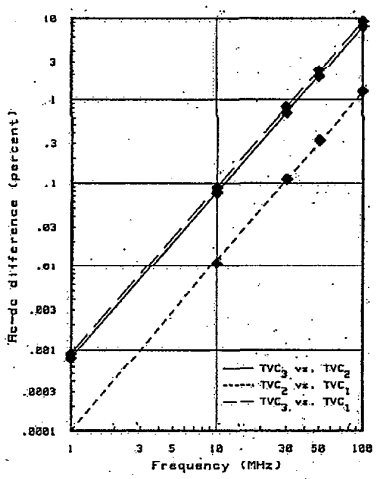

Fig. 5. Calculated values for series resistor transimpedance contribution to ac–dc difference shown as solid and dashed lines for three pairs of TVC's. Measured points shown as diamonds.

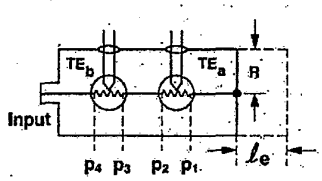

Fig. 6. Arrangement for intercomparison of thermoelements in series using split cylinder

where

$$k = \frac{L_u C_u}{2} = \frac{\epsilon_0 \mu_0}{2} = 0.56 \times 10^{-21}$$

for x in centimeters.

Note that for the conditions given above, the ratios of the center conductor diameter to the diameter of the outer cylinder cancel out in the expression for k.

The lengths of the TE heaters, p_1-p_2 and p_3-p_4 in Fig. 6, were short compared to the length of the overall structure. The power dissipated in the heater was, therefore, taken to be the current at the thermocouple position, squared, times the heater resistance. Integration of the current over the short length of heater yields essentially the same numerical results. The power H in a TE at position x is:

$$H = R_h I_x^2 \simeq R_h I_r^2 (1 - 2k\omega^2 x^2).$$

It can be shown that the relative ac–dc difference δ_r due to the current standing wave for the two thermoelements, TE_a and TE_b, in series in the split cylinder is

$$\delta_r = \frac{H_b - H_a}{2H_a} \simeq k\omega^2 (x_b^2 - x_a^2). \qquad (3)$$

This analysis assumes a perfect short circuit at $x = 0$. For both the split cylinder and the TVC structure, the end plates were suspected to be imperfect short circuits. The result of such an imperfect short is an extension in the effective electrical length l_e of the transmission line. The value for l_e can be determined by graphical means or by an estimation and iteration method, as was used for this determination. Using the measured relative values of ac–dc difference at 100 MHz for two TE's in the split cylinder with the locations of TE_b and TE_a as 6.84 cm and 3.38 cm and $R = 2.5$ cm, the value of $l_e = 3.68$ cm was obtained. The effectiveness of this analysis and the justification for the use of the same l_e value over the whole frequency range may be seen from Fig. 7 which shows the measured data points (diamonds) and the values predicted by the analysis using l_e as determined at 100 MHz (dashed line).

The same type of expression and the value of l_e were used to relate the power in a TE, mounted in a TVC, to the current flowing out of the series resistor. The ac–dc difference contributions of the current standing wave in the TE were calculated using values for the distance from the physical end of the cylinder to the TE and to the resistor of 1.27 and 4.19 cm, respectively, and are given in Section VI.

IV. Frequency Region of 0.1–1 MHz

In the region of 0.1–1 MHz, the range-independent contributions to ac–dc difference, namely standing wave in the connector and tee structure and current standing wave in the TE are, as shown above, quite small and generally negligible compared to the random uncertainty. Of the two remaining range-dependent contributions, the skin effect and reactance may be considered in terms of the transimpedance Z and the dc resistance R_{dc} in the calculation of ac–dc difference δ:

$$\delta = \frac{|Z| - R_{dc}}{R_{dc}}$$

where

$$|Z| = (R_{ac}^2 + X^2)^{1/2}$$

$$R_{ac} = R_{dc} + R_s$$

where R_s is the addition to resistance from skin effect. If $X \ll R_{dc}$ and $R_s \ll R_{dc}$, $\delta \approx \frac{1}{2}(X/R_{ac})^2 + R_s/R_{dc}$ (with higher order terms neglected). Converters of different ranges were constructed with very similar geometry from cylinders and resistors of the same physical size and shape. Resistors with different values ranging from 1 to 5 kΩ were matched with TE's of different heater current ratings to form converter modules with voltage ratings of 10–25 V. For a pair of such converters made from similar materials and with very similar geometry, but with series resistance values different by more than two to one, the geometric reactance and skin effect contributions would be easily detectable if they were large enough to be significant, but they were observed to be quite small, as shown below.

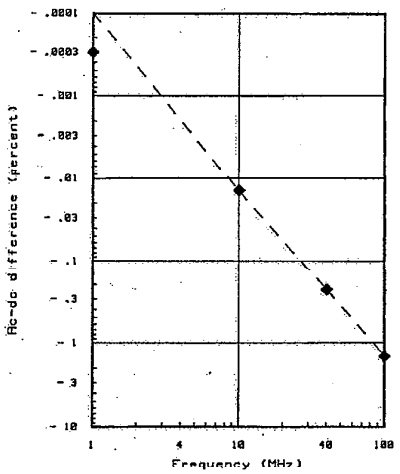

Fig. 7. Calculated values for contribution to ac–dc difference due to the current standing in the thermoelement shown as the dashed line. Measured points shown as diamonds.

Additional range-independent ac–dc difference contributions may arise from the thermoelement. Two sources of ac–dc difference in common were skin effect in the heater and dielectric loss in the bead. Intercomparisons showed that the ac–dc differences of the TE's as current converters were equal to within 5 ppm. Consistent with these measurements, a calculation of the skin effect [2, pp. 30–37] (one possible source of ac–dc difference as a current converter) for a 100-Ω heater [2, pp. 30–37] gave a change in resistance of 30 ppm at 100 MHz and decreasing at lower frequencies proportional to $\sqrt{F}$. The effect of dielectric loss in the bead was tested using two TE's connected in series in a single enclosure. By placing a series resistor between the two heaters the voltage across one bead could be varied. This test showed no significant ac–dc difference contribution due to dielectric loss in the bead for the TE's under study over the 0.1–100 MHz frequency range.

To test the relationship and arguments described above, three special midrange TVC's were studied in the voltage range of 10–25 V for which the variations in ac–dc difference contributions over the 0.1–1 MHz frequency range should be minimized. The results of intercomparisons between pairs of these TVC's at 0.1, 0.2, 0.5, and 1 MHz, respectively, are given in Table I. The TVC listed on top was taken as the test converter in each case. The intercomparisons of the three pairs of TVC's do not sum to zero around the loop, and the values for these failures to close the loop are also given in Table I. In conjunction with comparisons against the National Bureau of Standards (NBS) low frequency standard thermal voltage converters [4] at 100 kHz, which are given as the first column

TABLE I
AC-DC DIFFERENCE INTERCOMPARISONS (PPM), FREQUENCY (MHz)

	0.1	0.2	0.5	1
C 25 - 5 k vs C 10 - 1 k	+4	+6	+3	+6
C 25 - 5 k vs C 10 - 2 k	+5	+2	+7	+8
C 10 - 2 k vs C 10 - 1 k	+3	+2	0	+1
Failure to Close	4	2	4	3

TABLE II
ASSIGNED AC-DC DIFFERENCE VALUES (PPM), FREQUENCY (MHz)

	0.1	0.2	0.5	1
C 10 - 1 k	-8	-8	-8	-8
C 10 - 2 k	-5	-6	-8	-7
C 25 - 5 k	-4	-2	-5	-2

in Table II, these results provide the basis for the frequency extension of 0.1 to 1 MHz.

Values were assigned to these three special TVC's by taking C10–1 k to be frequency independent, and the results are given in Table II. Very little change would result from taking C10–2 k as frequency independent or from dividing the difference between C10–1 k and C10–2 k.

V. Skin Effect

For lower voltage range TVC's having smaller series resistors, the skin effect may be significant in the 1 MHz region. As shown in Terman [2, pp. 30–37], when the quantity χ (proportional to frequency/resistance) is sufficiently low for a particular set of conditions, then the increase in resistance due to skin effect is proportional to the permeability (μ) and frequency (f) squared. As the factor χ becomes larger, the increase in resistance due to skin effect becomes proportional to $(f\mu)^{1/2}$. The replacement of part of a nonmagnetic structure with a magnetic material produces an enhanced change in resistance due to skin effect. A group of special tests was performed to confirm that the skin effect contribution for the principal TVC's under study was quite small. The effect of magnetic leads and feedthroughs on the thermoelement was determined by comparing a TVC, constructed with a 5-mA TE having dumet leads, to a reference TVC, and then carefully replacing the TE by one having nonmagnetic platinum iridium leads and feedthroughs. The changes in ac–dc difference due to magnetic leads on the TE were found to be less than 3 ppm for a 10 V TVC with a 2-kΩ series resistor for frequencies of 0.1–1 MHz.

As mentioned above, the series resistors originally had magnetic end caps and leads which were replaced with copper end caps and copper leads. The original and modified constructions are shown in Fig. 2. The changes in ac–dc difference which resulted from replacement of the end caps and leads are given in Table III. These measurements, and the ones described for the magnetic TE leads, were used to calculate the skin effect magnitude for lower range TVC's containing resistors with magnetic end caps and thermoelements made with magnetic dumet leads. The changes in absolute resistance represented by the ac–dc differences assigned to the magnetic materials were used with the particular range resistance values to determine the values reported below in the results section.

TABLE III
CHANGE IN AC-DC DIFFERENCE (PPM) DUE TO REPLACEMENT OF RESISTOR END CAPS AND LEADS FOR A 10-V TVC WITH 2-kΩ SERIES RESISTOR, FREQUENCY (MHz)

0.1	0.2	0.3	0.5	1 MHz
-4	-5	-6	-8	-10

At frequencies above 1 MHz the skin effect contribution for the TVC's under study becomes less important relative to reactive and transmission line effects due to the $(f\mu)^{1/2}$ dependence for the former and $(f\mu)^2$ dependence for the latter. Using the method suggested by Huang [5], coefficients for the $(f\mu)^{1/2}$ and $(f\mu)^2$ terms were determined at frequencies above 1 MHz for particular pairs of TVC's made with resistors and thermoelements containing some magnetic material. Calculations of the coefficients using different frequency pairs (e.g., 10–50 MHz 10–70 MHz, 10–100 MHz) gave results in agreement to within 1–2 percent for both the $f^{1/2}$ and f^2 terms. These coefficients were used to calculate the skin effect contribution for the C3 and C5 converters given in the results section.

VI. Results

Each contribution to the overall ac–dc difference has been determined from calculations and measurements for several TVC's. Tables IV–VIII give five examples of the detailed breakdown for the individual elements, namely skin effect δ_s, transimpedance of series resistor δ_{tr}, voltage standing wave in input connection δ_c, and current standing wave in thermoelement δ_{swr}. Note that the TVC's marked C10 and C10B are different from TVC_1 and TVC_2 of Fig. 5. The converters labeled C3 and C5 did contain resistors with magnetic end caps and leads as well as thermoelements with magnetic dumet leads. The characterizations at 1 MHz and below do not rely solely on the values of δ_s which were determined as outlined in the skin effect section above. These values of δ_s are included as an indication of how well this model describes these low voltage TVC's in this frequency range and were used as the starting point for high frequency skin effect estimates using the $f^{1/2}$ relation described above.

As part of a cooperative effort with G. Rebuldela in the NBS Electromagnetic Fields Division, Boulder, CO, the ac–dc differences for these and other TVC's were also de-

TABLE IV
AC-DC DIFFERENCE (PERCENT), CONVERTER C3, 3 V, 500-Ω SERIES RESISTOR

	1 MHz	10 MHz	30 MHz	50 MHz	100 MHz
δ_s	+0.006	+0.019	+0.033	+0.041	+0.061
δ_{tc}	0	-0.002	-0.015	-0.042	-0.17
δ_c	0	-0.012	-0.11	-0.30	-1.18
δ_{swr}	0	-0.0083	-0.075	-0.21	-0.83
Calculated Total δ	+0.006	-0.003	-0.17	-0.51	-2.12
Measured† δ	+0.006*	-0.057	-0.18	-0.54	-2.43

* 1 MHz values measured in terms of TVC's characterized as described in the 0.1 - 1 MHz section of this paper.

† 10, 30, 50, and 100 MHz values measured in terms of NBS Boulder calibrated TVC's.

TABLE V
AC-DC DIFFERENCE (PERCENT), CONVERTER C5, 5 V, 1000-Ω SERIES RESISTOR

	1 MHz	10 MHz	30 MHz	50 MHz	100 MHz
δ_s	+0.003	+0.011	+0.019	+0.024	+0.034
δ_{tc}	0	-0.003	-0.025	-0.070	-0.28
δ_c	0	-0.012	-0.11	-0.30	-1.18
δ_{swr}	0	-0.0083	-0.075	-0.21	-0.83
Calculated Total δ	+0.003	-0.012	-0.19	-0.56	-2.26
Measured† δ	+0.002*	-0.051	-0.20	-0.58	-2.52

* 1 MHz values measured in terms of TVC's characterized as described in the 0.1 - 1 MHz section of this paper.

† 10, 30, 50, and 100 MHz values measured in terms of NBS Boulder calibrated TVC's.

TABLE VI
AC-DC DIFFERENCE (PERCENT), CONVERTER C10, 10 V, 2-kΩ SERIES RESISTOR

	1 MHz	10 MHz	30 MHz	50 MHz	100 MHz
δ_s	+0.001	+0.004	+0.007	+0.008	+0.012
δ_{tc}	0	+0.005	+0.046	+0.13	+0.51
δ_c	0	-0.012	-0.11	-0.30	-1.18
δ_{swr}	0	-0.0083	-0.075	-0.21	-0.83
Calculated Total δ	+0.001	-0.011	-0.13	-0.37	-1.49
Measured † δ	0*	-0.049	-0.14	-0.40	-1.75

* 1 MHz values measured in terms of TVC's characterized as described in the 0.1 - 1 MHz section of this paper.

† 10, 30, 50, and 100 MHz values measured in terms of NBS Boulder calibrated TVC's.

termined by comparison with converters calibrated at the NBS Boulder Laboratories. The Boulder calibrations were based on characterizations using a bolometer bridge [6] and later reconfirmed by applied power and input impedance determinations [7]. The uncertainties for the NBS Boulder calibrations were 0.1 percent at 10 MHz, 0.2 percent at 30 MHz, and 1 percent at 100 MHz. The results of these tests are given as the measured values in Tables IV–VIII. Although the variations at 10 MHz between this

TABLE VII
AC-DC DIFFERENCE (PERCENT), CONVERTER C10B, 10 V, 2.1-kΩ SERIES RESISTOR

	1 MHz	10 MHz	30 MHz	50 MHz	100 MHz
δ_s	0	0	+0.001	+0.001	+0.001
δ_{tc}	0	+0.005	+0.054	+0.15	+0.60
δ_c	0	-0.012	-0.11	-0.30	-1.18
δ_{swr}	0	-0.0083	-0.075	-0.21	-0.83
Calculated Total δ	0	-0.014	-0.13	-0.36	-1.41
Measured† δ	-0.001*	-0.052	-0.13	-0.39	-1.63

* 1 MHz values measured in terms of TVC's characterized as described in the 0.1 - 1 MHz section of this paper.

† 10, 30, 50, and 100 MHz values measured in terms of NBS Boulder calibrated TVC's.

TABLE VIII
AC-DC DIFFERENCE (PERCENT), CONVERTER C25, 25 V, 5.6-kΩ SERIES RESISTOR

	1 MHz	10 MHz	30 MHz	50 MHz	100 MHz
δ_s	0	+0.001	+0.001	+0.002	+0.002
δ_{tc}	+0.001	+0.084	+0.76	+2.1	+8.4
δ_c	0	-0.012	-0.11	-0.30	-1.18
δ_{swr}	0	-0.0083	-0.075	-0.21	-0.83
Calculated Total δ	+0.001	+0.065	+0.58	+1.59	+6.39
Measured δ	-0.001*	+0.024	+0.56	+1.53	+6.24

* 1 MHz values measured in terms of TVC's characterized as described in the 0.1 - 1 MHz section of this paper.

† 10, 30, 50, and 100 MHz values measured in terms of NBS Boulder calibrated TVC's.

work and the values measured in terms of the NBS Boulder calibrations are well within the Boulder uncertainties given above, further study is planned at this frequency. The fact that the results show generally excellent agreement between two entirely different methods makes it very unlikely that any significant contribution to ac–dc difference has been omitted.

VII. Uncertainty of Characterization

All of the significant known contributions to overall ac–dc difference for the particular TVC's under study for this project are itemized along with estimated uncertainties, corresponding to one standard deviation, in Table IX. In the case of certain items, namely range resistor transimpedance, current standing wave in TE, and the voltage standing wave in the connector and tee, the uncertainty was estimated from the comparison of calculated and measured values. Significant to the estimation of the uncertainty for the current standing wave contribution was the high sensitivity of this effect to dimensional measurements required in the determination of l_e, and subsequently δ_{SWR}. The comparison system uncertainty was estimated from repeatability of results after making variations to the physical arrangements. The uncertainty

TABLE IX
UNCERTAINTY ESTIMATES (PPM)

	1 MHz	10 MHz	30 MHz	100 MHz
Thermoelement as current converter	3	10	30	300
Transimpedance of series resistor	5	15	50	500
Current standing wave in thermoelement	5	30	100	1000
Comparison process standard deviation	6	10	10	20
Comparator system uncertainty	3	10	30	100
Tee and connector standing wave	3	15	50	500
Connector reproducibility	3	10	30	300
Skin Effect	3	10	20	40
100 kHz determination	7	7	7	7
Square root of the sum of the squares	13	44	135	1301
Estimated uncertainty corresponding to one standard deviation	20	80	300	2000

of the TE as a current converter was based on the reproducibility of the mounting for the tests. The skin effect uncertainty estimate was based on calculated and measured values, and the connector defect contribution was determined from tee inversions and repeated plugging and unplugging. The estimated uncertainties were combined by the square root of the sum of the squares (RSS) method. These RSS values and the estimated overall uncertainties, corresponding to the one standard deviation confidence level, are given at the bottom of the Table IX.

ACKNOWLEDGMENT

The authors acknowledge and express appreciation for the considerable advice and encouragement given by F. L. Hermach, consultant to the NBS Electricity Division. Acknowledgment and appreciation are also given to G. Rebuldela, NBS Electromagnetic Fields Division, for supplying important data on several TVC's; to D. Stollery, Thermal Techniques Ltd., for the fabrication of special thermoelements; to S. Fromm, for manuscript preparation; and to T. E. Lipe, NBS Electricity Division, for assistance with computer software and graphics.

REFERENCES

[1] F. L. Hermach and E. S. Williams, "Thermal voltage converters for accurate voltage measurements to 30 megacycles per second," *Trans. AIEE (Comm. Electron.)*, vol. 79, pp. 200–206, July 1960.
[2] F. E. Terman, *Radio Engineers' Handbook*. New York, N.Y.: McGraw-Hill, 1943.
[3] D. R. Crosby and C. H. Pennypacker, "Radio-frequency resistors as uniform transmission lines," in *Proc. IRE*, vol. 34, pp. 62–66, Feb. 1946.
[4] F. L. Hermach, "An investigation of the uncertainties of the NBS thermal voltage and current converters," Nat. Bur. Stand. Gaithersburg, MD, Rep. NBSIR 84-2903, Apr. 1985.
[5] D.-X. Huang, "RF coaxial thermal transfer standard," in *CPEM '86 Dig.*, 1986, pp. 223–224.
[6] M. C. Selby and L. F. Behrent, "A bolometer bridge for standardizing radio-frequency voltmeters," *J. Res. Nat. Bur. Stand.*, vol. 44, pp. 15–30, Jan. 1950.
[7] G. Rebuldela, "RF voltmeter calibration services," Nat. Bur. Stand. Boulder, CO, Tech. Note, in preparation.